J Therm Anal Calorim
DOI 10.1007/s10973-017-6617-5

Thermal decomposition characteristics of microwave liquefied rape straw residues using thermogravimetric analysis

Xingyan Huang[1,2] · Cornelis F. De Hoop[1] · Jiulong Xie[1,2] · Chung-Yun Hse[3] · Jinqiu Qi[2] · Yuzhu Chen[2] · Feng Li[2]

Received: 31 January 2017 / Accepted: 26 July 2017

Abstract The thermal decomposition characteristics of microwave liquefied rape straw residues with respect to liquefaction condition and pyrolysis conversion were investigated using a thermogravimetric (TG) analyzer at the heating rates of 5, 20, 50 °C min^{-1}. The hemicellulose decomposition peak was absent at the derivative thermogravimetric analysis (DTG) curve of liquefied residues, because it had been decomposed during the liquefaction. Furthermore, among the liquefied residues, the one from the reaction condition of 180 °C/15 min had the highest thermal stability under a high temperature (>700 °C). The DTG profiles revealed that raising the temperature heating rate could result in an increase in the maximum decomposition temperature. The apparent activation energy (E_α) values of the liquefied residues were lower than that of non-liquefied raw rape straw, whereas the recondensation reaction occurred at 180 °C/15 min remarkably increased the E_α. A noticeable increase in the E_α was observed for the liquefied residue from the 180 °C/10 min samples as the pyrolysis conversion increased from 0.15 to 0.55, suggesting a complex decomposition process with the increasing pyrolysis temperature. The liquefaction process could decrease the thermal decomposition temperature of biomass, which means higher reactivity and lower operational costs during pyrolysis.

Keywords Thermogravimetry · Liquefied residue · Rape straw · Microwave

Introduction

With the growing concern of environmental protection and rapid depletion of fossil fuel, the utilization of lignocellulosic biomass, a type of degradable and renewable resource, has attracted an increasing worldwide attention. Specially, in China, a large quantity of rape straw is produced annually as agro-waste. Liquefaction is one of the widely investigated methods to convert lignocellulosic biomass into valuable chemicals of fuels in recent years [1, 2]. Through liquefaction, the high molecular weight components of biomass are broken down to low molecular weight gases, liquids and liquefied residues. Generally, the gases are omitted because the yield of gaseous products is negligible. The liquid portion is the most commonly utilized liquefaction product. It can be applied to produce wood adhesive [3], bio-based polyurethane foam [4], methyl levulinate [5], etc. However, there are a few reports about the utilization of the liquefied residues. The conventional one is to add it into polymer composites as a reinforcing agent [6]. The latest utilization method is to isolate cellulose nanofiber from liquefied residues [7, 8]. A potential utilization method of the liquefied residue should be to pyrolyze it into value added products.

Pyrolysis is one of the promising thermochemical conversion routes, playing an important role in biomass conversion. The end products of pyrolysis of gases and liquids

✉ Cornelis F. De Hoop
cdehoop@lsu.edu

✉ Jiulong Xie
jxie6@lsu.edu

[1] School of Renewable Natural Resources, Louisiana State University Agricultural Center, Baton Rouge, LA 70803, USA

[2] College of Forestry, Sichuan Agricultural University, Chengdu, Sichuan 611130, People's Republic of China

[3] Southern Research Station, USDA Forest Service, Pineville, LA 71360, USA

Published online: 17 August 2017

can be used as fuel due to their high calorific value [9, 10]. Information on pyrolysis kinetics is vital to evaluate biomass as a feedstock for fuel or chemical production. It is also crucial in the control of thermochemical conversion processes [11]. The study of the thermal decomposition characteristics of condensed wood liquefied residues was used to clarify the condensation reaction mechanism during liquefaction [12]. The evaluation on pyrolysis properties of agro-waste, such as corn stalk, can be found in previous study [13]. However, there is no study on the thermal decomposition characteristics of liquefied residues from agro-waste. Therefore, it is essential to study the fundamentals of thermal decomposition properties of the liquefied rape straw residue.

Thermogravimetric analysis (TG) can quantify mass change and thermal decomposition of the samples [14]. It has been extensively used in the research on pyrolysis of biomasses, such as polar wood [14], corn stalk [15], macroalgae [16] microalgae [17], cellulose nanofibers and nanowhiskers [18], tar from gasification [19], and pseudocomponents of biomass (i.e., cellulose, hemicelluloses and lignin) [20]. These studies help clarify our understanding of pyrolysis kinetic.

The main chemical components in biomass including hemicellulose, lignin and cellulose are the basic factors to interpret the pyrolysis properties. A previous study indicated that the mass loss of hemicellulose, cellulose and lignin mainly happened at 220–315, 315–400 and 160–900 °C, respectively [21]. However, hemicellulose is the most susceptible chemical component to liquefaction, followed by the lignin and cellulose [22]. Therefore, the main chemical components in liquefied residues will be inhomogeneity with the change in liquefaction conditions. It will result in the difference of pyrolysis properties of liquefied residues from different liquefaction conditions.

Thus, in this study, the thermal decomposition characteristics of microwave liquefied residues from different liquefaction conditions were investigated using thermogravimetric analysis at three different heating rates (5, 20, 50 °C min^{-1}) under an inert nitrogen atmosphere. Kinetic parameters, including apparent activation energy (E_α) and pre-exponential factor (expressed as ln A_α), were determined by the model reported by Kissinger 1957 [23]. The pyrolysis properties of liquefied residue with conversion were also studied using the Kissinger method to provide fundamental pyrolysis parameters for the integrated utilization of liquefied residue.

Methods

Materials

Rape straw from Sichuan province (Southwest of China) was milled in a knife mill to pass through a 20-mesh and maintain in 40-mesh sieve. Then, the milled sample was oven-dried at 105 °C until constant weight. The holocellulose, α-cellulose, lignin content, alcohol-toluene extractives and ash content of raw rape straw were determined according to ASTM standards D 1104-56 (1971), D 1103-60 (1971), D 1106-96 (1996), D 1107-96 (1996) and ASTM D 1102-84 (2001), respectively. The hemicellulose content was established in accordance with the method reported in previous study [24]. The chemical components of rape straw were as following: α-cellulose (36.72%), hemicellulose (32.67%), Klason lignin (13.66%), alcohol-toluene extractives (4.46%), and ash content (8.27%). All reagent grade chemicals, including sulfuric acid (95–98%) and methanol, were purchased from commercial sources and used without further purification.

Microwave liquefaction

Liquefaction of rape straw was performed in a Milestone MEGA laboratory microwave oven (Shelton, CT, USA) equipped with an ATC-400FO automatic fiber-optic temperature control system. A typical run was carried out with a loading of 2 g of rape straw, 12 g of methanol and 0.36 g of sulfuric acid, i.e., so that the concentration of H_2SO_4 was 3%. The mixed reactants were sealed in a 100-mL Teflon reaction vessel with a magnetic stirring bar. The output power of the microwave energy was auto-adjusted based on the temperature feedback from the sensor under maximum power of 700 W. The sealed vessels were subjected to microwave irradiation. The reaction temperature was increased from room temperature to the desired temperature (i.e., 140, 160 and 180 °C) within 5 min, and then maintained for 2.5, 5 or 10 min. An ice bath was applied to quench the reaction when it was done. After cooling, the liquefied products were dissolved in 150 mL of methanol under constant stirring for 4 h and filtered through Whatman No. 4 filter paper to separate the liquid and the solid residue. The solid residue contents from a series of liquefaction conditions are shown in Table 1.

Thermogravimetric analysis

The TG analysis measurements of raw rape straw and liquefied residues (Fig. 1) were conducted with a thermal analyzer Q50 TG (TA Instruments, New Castle, DE, USA) to simultaneously obtain thermogravimetric data. As the

Table 1 Solid residue contents with respect to liquefaction condition

Liquefaction conditions	140 °C/15 min	160 °C/15 min	180 °C/7.5 min	180 °C/10 min	180 °C/15 min
Residue content/%	44.22	30.15	23.44	13.46	16.78

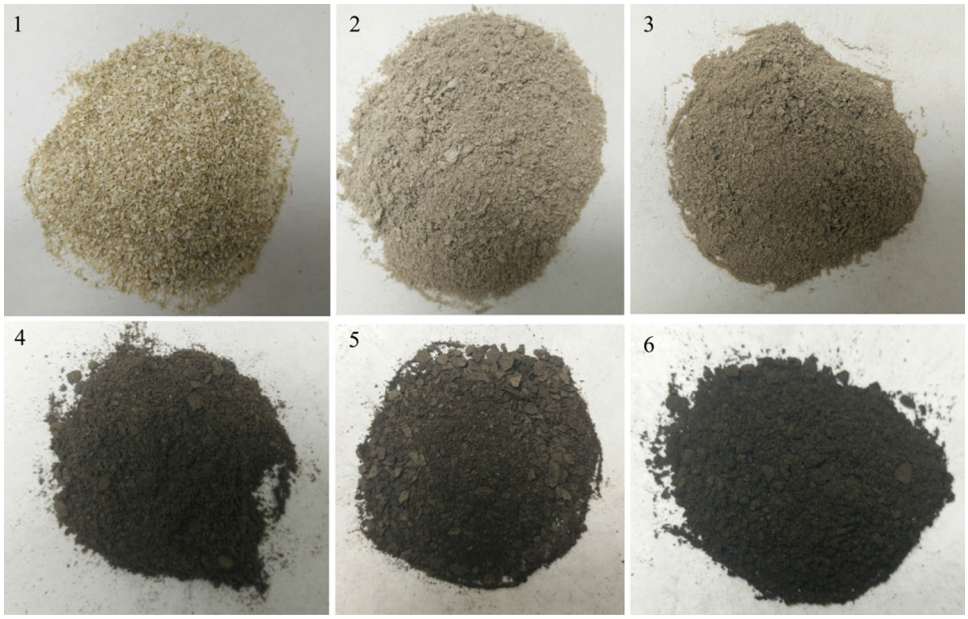

Fig. 1 Raw material and liquefied rape straw residues (*1*: rape straw; *2*: 140 °C/15 min; *3*: 160 °C/15 min; *4*: 180 °C/7.5 min; *5*: 180 °C/10 min; *6*: 180 °C/15 min)

potential purpose of this study is to explore the pyrolysis utilization of liquefied residues instead of its combustion properties, the TG analysis was only performed under an inert nitrogen atmosphere. Each sample, about 3 mg, was placed in a platinum pan and then heated from 30 to 800 °C with constant heating rates of 5, 20 and 50 °C min^{-1} under a flow of 40 mL min^{-1} of high-purity nitrogen atmosphere (99.999%).

Non-isothermal thermogravimetric kinetics

In this study, α is defined as the conversion of sample expressed as normalized mass loss of decomposed sample, as Eq. 1,

$$\alpha = \frac{W_o - W_t}{W_o - W_f} \tag{1}$$

where W_o is the initial sample mass, W_t represents the actual mass at time t and W_f stands for the final sample mass after pyrolysis.

The conversion rate of solid sample to volatile product is commonly based on a single-step kinetic equation [19, 25], as Eq. 2,

$$\frac{d\alpha}{dt} = k(T_i)f(\alpha) \tag{2}$$

where $d\alpha/dt$, t, T_i, $k(T_i)$ and $f(\alpha)$ are the conversion rate, time, absolute temperature, rate coefficient and the reaction model, respectively. $k(T_i)$ and $f(\alpha)$ are determined as Eqs. 3 and 4, respectively.

$$k(T_i) = A_\alpha \exp\left(-\frac{E_\alpha}{RT_i}\right) \tag{3}$$

where A_α is the pre-exponential factor (min^{-1}), R is the gas constant (8.314 J K^{-1} mol^{-1}) and E_α is the activation energy (kJ mol^{-1}).

$$f(\alpha) = (1-\alpha)^n \tag{4}$$

where n is the reaction order. The most common reaction models for solid-state kinetic are organized in four categories that are nucleation, geometrical, diffusion and reaction order. The detailed description of reaction order was reported by Tadini et al. [26].

Combining Eqs. 2, 3 and 4, the reaction rate can be written as Eq. 5,

$$\frac{d\alpha}{dt} = A_\alpha \exp\left(-\frac{E_\alpha}{RT_i}\right)(1-\alpha)^n \tag{5}$$

The constant heating rate β is expressed as Eq. 6,

$$\beta = \frac{dT_i}{dt} \tag{6}$$

As the conversion rate is a function of temperature, and the temperature is related to the heating time, the conversion rate can be described by Eq. 7,

$$\frac{d\alpha}{dt} = \frac{d\alpha}{dT_i}\frac{dT_i}{dt} = \beta\frac{d\alpha}{dT_i} \quad (7)$$

Substituting expression (7) into Eq. 6, the sample decomposition can be expressed as Eq. 8,

$$\frac{d\alpha}{dT_i} = \frac{A_\alpha}{\beta}\exp\left(-\frac{E_\alpha}{RT_i}\right)(1-\alpha)^n \quad (8)$$

A model-free non-isothermal function is obtained by transforming Eq. 9 in accordance to the method reported by Kissinger 1957.

$$\ln\left(\frac{\beta}{T_i^2}\right) = \ln\left(\frac{A_\alpha R}{E_\alpha}\right) - \frac{E_\alpha}{RT_i} \quad (9)$$

Model-fitting and model-free methods are used to obtain the thermal degradation kinetic parameters under non-isothermal conditions. The former is insufficient in kinetic studies due to the limited applicability of single heating rate data, whereas the model-free approach based on multi-heating rates and isoconversional data is more helpful in the study of kinetic parameters [19, 27, 28].

The most used methods mentioned in previous publications to calculate the kinetic parameters are Ozawa–Flynn–Wall (OFW), Kissinger, Kissinger–Akahira–Sunose (KAS), and Starink [15, 26, 29]. The OFW provides the lowest accuracy because it is based on a crude approximation, while the others could give more accurate kinetic parameters [26]. The Kissinger method was used previously to study thermal degradation kinetics of liquefied residues [12]. It is also recommended by the Kinetics Committee of the International Confederation for Thermal Analysis and Calorimetry (ICTAC) for conducting kinetics computation on thermal analysis data [16]. In the present study, the classic Kissinger method was only considered to be used as the computational method to calculate the activation energy and the pre-exponential factor by plotting $\ln(\beta/T_i^2)$ against $1/T_i$ for different liquefaction conditions or different pyrolysis conversions (α). The E_α and A_α can be obtained from the slope and intercept of a straight line [30].

Results and discussion

Thermal decomposition characteristics

The thermogravimetry/derivative thermogravimetric analysis (TG/DTG) curves of the raw rape straw and liquefied residues are shown in Figs. 2 and 3. The first stage of mass loss (<150 °C) was attributed to the removal of absorbed moisture and light volatile components. After this peak, the DTG cure of raw rape straw showed three decomposition regimes: (1) the first decomposition shoulder peak at about 180–275 °C was attributed to thermal depolymerization of

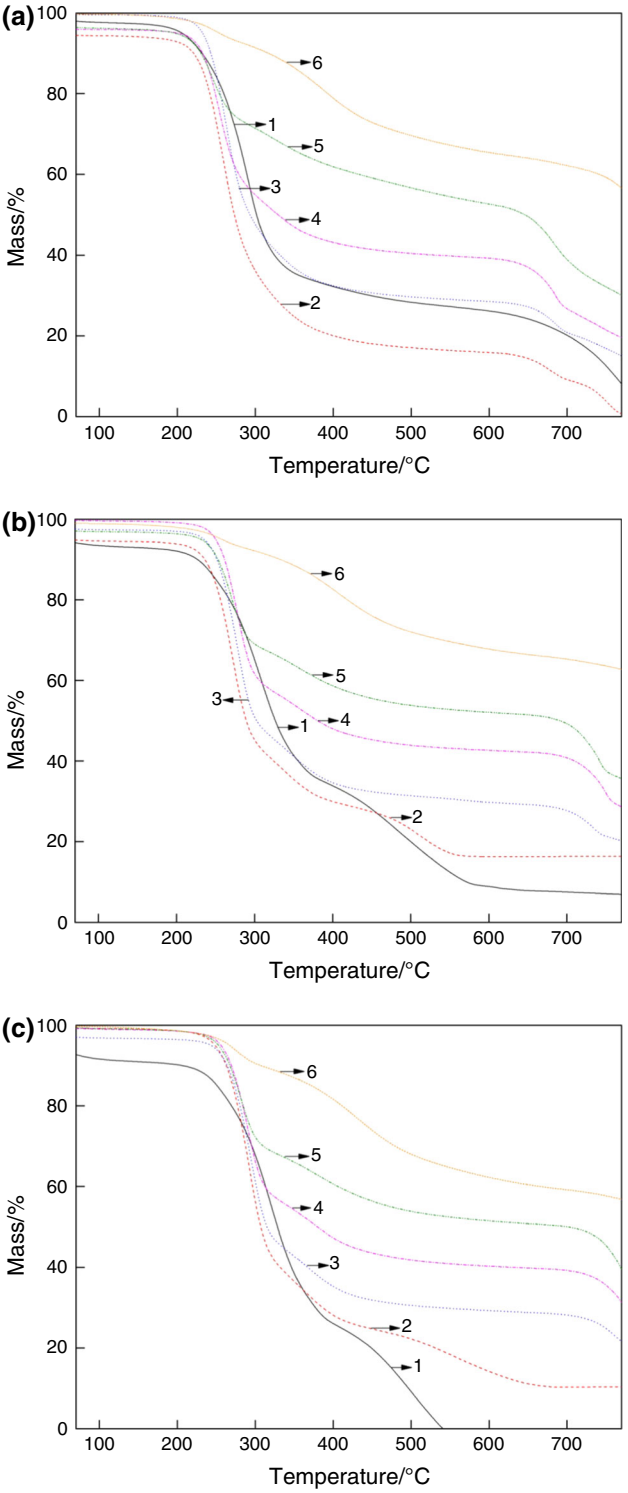

Fig. 2 TG curves of rape straw and liquefied residues from different liquefaction conditions at the heating rate of 5 °C min^{-1} (**a**), 20 °C min^{-1} (**b**), and 50 °C min^{-1} (**c**) (*1*: rape straw; *2*: 140 °C/15 min; *3*: 160 °C/15 min; *4*: 180 °C/7.5 min; *5*: 180 °C/10 min; *6*: 180 °C/15 min)

hemicelluloses or pectin; (2) the primary decomposition peak in the temperature range of 280–390 °C corresponded to cellulose decomposition [21]; (3) peak from 410 to

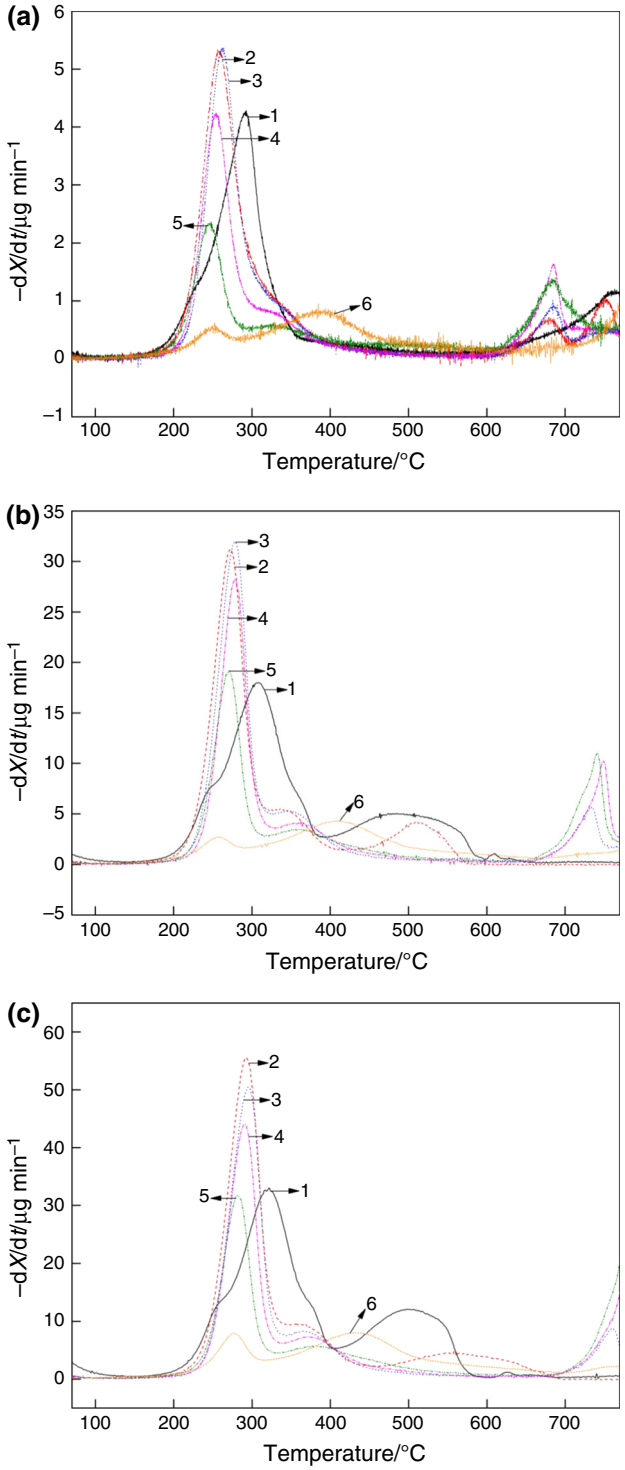

Fig. 3 DTG curves of rape straw and liquefied residues from different liquefaction conditions at the heating rate of 5 °C min^{-1} (**a**), 20 °C min^{-1} (**b**), and 50 °C min^{-1} (**c**) (*1*: rape straw; *2*: 140 °C/15 min; *3*: 160 °C/15 min; *4*: 180 °C/7.5 min; *5*: 180 °C/10 min; *6*: 180 °C/15 min)

585 °C corresponded to lignin degradation [9]. As compared with raw rape straw, liquefied residues lacked the shoulder peak corresponding to the hemicellulose decomposition. This was explained by the removal of hemicellulose at the initial liquefaction stage because it is the most susceptive to liquefaction among the main chemical components of fiber cell wall [22]. Furthermore, all of the liquefied residues had lower maximum decomposition temperatures, as indicated from the shift of major DTG peaks to lower temperature in comparison with raw material, suggesting that liquefied residues have higher reactivity. Although lignin is susceptive to liquefaction and decompose easily during liquefaction [22], the DTG cure of liquefied residue from 140 °C/15 min presented a broad function peak of lignin at around 520 °C. This suggested that a little lignin remained in the liquefied residue.

Unlike the raw rape straw, the liquefied residues were observed to have a shoulder at about 350 °C, which is attributed to the degradation of α-cellulose [31], except for the one from 180 °C/15 min. There were a few of peaks (around 740 °C) presented on the DTG curves of the liquefied residues, but that from 180 °C/15 min. Those peaks might be attributed to the decomposition of charred residues. It could be the result of the breakdown of C–C and C–H bonds of the char [32]. A similar result was reported by Ceylan et al. [11]. This result suggested that the char obtained from 180 °C/15 min has the highest thermal stability under a high temperature (>700 °C). This was further evidenced by the higher char content in comparison with the ones from other liquefaction conditions. With the increasing of liquefaction temperature and time, the char at 770 °C, obtained from liquefied residue, increased remarkably regardless of the heating rate (Table 2). One possible reason was that the formation of insoluble substances at severe liquefaction conditions increased the thermal stability. It was demonstrated that the insoluble substance mainly consisted of humins and unreacted cellulose [33], or recondensation resultant of hemicellulose and lignin fragments [12]. The formation of insoluble substances also resulted in the increasing liquefied residue content, as shown in Table 1. Generally, the char content increased with the increasing of heating rate. It was attributed to the low thermal transfer efficiency at a high heating rate. This result was in agreement with a previous report [12]. A unique mass loss peak of liquefied residue at about 420 °C was observed from 180 °C/15 min. This might be attributable to the decomposition of a high degree of cellulose crystallinity. The removal of non-cellulose components during liquefaction could enhance the crystallinity index of cellulose and increase its thermal stability [6].

The maximum thermal decomposition rate and temperature somewhat decreased with the increase in liquefaction temperature and time. It was related to the difference of chemical components among liquefied residues. The decomposition of hemicellulose and lignin at the initial

Table 2 Thermal parameters of rape straw and liquefied residues obtained from TG analysis

Liquefaction residues	Heating rate/°C min^{-1}	Peak temperature/K	Maximum decomposition rate/μg min^{-1}	Char/%
Rape straw	5	565.92	4.24	8.16
	20	581.28	18.04	7.02
	50	595.37	33.06	–
140 °C/15 min	5	531.09	5.31	0.71
	20	545.77	31.04	16.38
	50	565.49	55.60	10.37
160 °C/15 min	5	535.34	5.34	14.64
	20	551.5	31.93	20.68
	50	569.13	50.37	22.11
180 °C/7.5 min	5	527.92	4.23	19.60
	20	552.80	28.16	28.65
	50	564.02	43.96	31.34
180 °C/10 min	5	518.96	2.32	30.08
	20	543.14	19.28	36.39
	50	555.05	31.46	39.53
180 °C/15 min	5	666.92	0.81	54.51
	20	682.69	4.24	65.16
	50	705.17	7.97	56.73

liquefaction stage contributed to the decrease in the maximum decomposition rate and temperature. As can be seen in Table 2, the maximum decomposition temperatures shifted to higher temperature zones when increasing the heating rate from 5 to 50 °C min^{-1}. The temperature resistance time in the samples shortened as the heating rate was increased, resulting in the retard of decomposition temperature [32]. Furthermore, the pool thermal conductivity of lignocellulosic biomass leads to a pool heat transfer [34]. The maximum thermal decomposition rate was also increased with the increase in heating rate. Ceylan and Topçu reported that the formation of volatile matter during hazelnut husk pyrolysis was slightly affected by the increasing heating rate [11]. Additionally, a higher heating rate would increase the activation energy for hemicellulose and cellulose and decrease that for lignin [8].

Non-isothermal thermogravimetric kinetics

The kinetic analysis parameters of raw rape straw and liquefied residues were determined by the Kissinger method in Eq. 9 (Table 3). Figure 4 depicted the linear regression of $\ln(\beta/T_i^2)$ versus $1/T_i$. Three maximum decomposition rate temperatures from DTG profiles corresponding to three heating rates were fitted to determine activation energy and pre-exponential factor. This approach has proven to be an effective way to calculate the

Table 3 Activation energy (E_α), pre-exponential factor ($\ln A_\alpha$) and coefficients (R^2) of rape straw and liquefied residues obtained by the Kissinger method

Liquefaction parameters	Fitted equation	E_α/kJ mol^{-1}	$\ln A_\alpha$/min^{-1}	R^2
Rape straw	$y = 33.63 - 25266.70x$	210.07	36.86	0.9933
140 °C/15 min	$y = 24.52 - 18759.21x$	155.96	27.45	0.9625
160 °C/15 min	$y = 25.82 - 19643.14x$	163.31	28.80	0.9826
180 °C/7.5 min	$y = 22.01 - 17409.75x$	144.74	24.86	0.9858
180 °C/10 min	$y = 21.73 - 16978.72x$	140.91	24.56	0.9904
180 °C/15 min	$y = 28.42 - 26448.53x$	219.89	31.69	0.9551

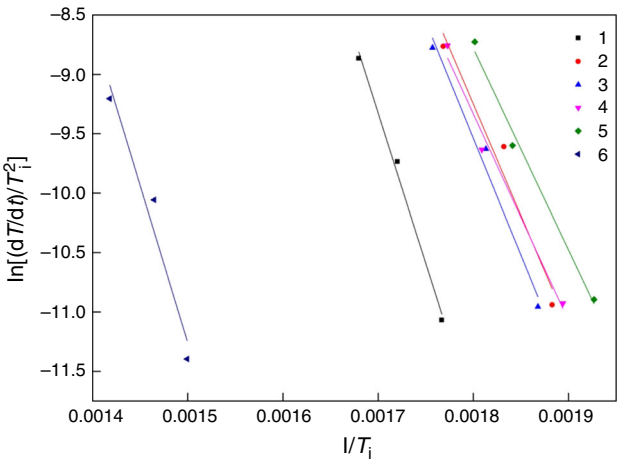

Fig. 4 Kissinger plots of rape straw and liquefied residues (*1*: rape straw; *2*: 140 °C/15 min; *3*: 160 °C/15 min; *4*: 180 °C/7.5 min; *5*: 180 °C/10 min; 6: 180 °C/15 min)

thermal degradation kinetic parameters from various materials [12]. Since the kinetic parameters were calculated from the maximum decomposition temperatures, the peak of lignin at around 520 °C observed from the DTG cure of liquefied residue from 140 °C/15 min would not affect the results of activation energy and pre-exponential factor. The coefficients (R^2) corresponded to linear regression in Fig. 4 were in the range of 0.955–0.993.

A reaction with higher E_α requires a higher energy to break down chemical bonds and results in a slower reaction [34]. As presented in Table 3, the E_α of raw rape straw was higher than those for liquefied residues except for 180 °C/15 min. The E_α of liquefied residues increased slightly at first from 155.96 to 163.31 kJ mol^{-1} with the increase in temperature from 140 to 160 °C for 15 min and then decreased to 140.91 kJ mol^{-1} as the liquefaction condition was changed to 180 °C/10 min. Finally, the E_α for 180 °C/

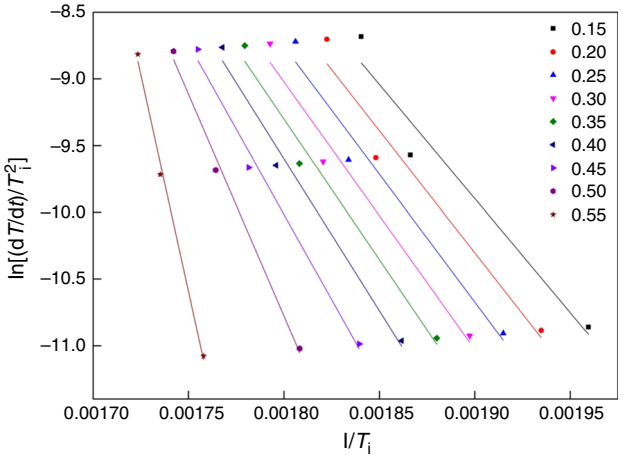

Fig. 5 Kissinger plots of liquefied residue from reaction condition of 180 °C/10 min at different pyrolysis conversion

15 min noticeably increased to 219.89 kJ mol^{-1}. This suggests that liquefying residue at 180 °C/10 min is preferable over other liquefaction conditions, because it requires the lowest activation energy.

The decomposition of hemicellulose, lignin and cellulose during liquefaction undermined the thermal stability of liquefied residues; thus, the E_α of liquefied residues reduced as compared with raw rape straw. In contrast, the recondensation reaction occurring at 180 °C/15 min enhanced the thermal stability and hence increased the E_α. Therefore, the increase in E_α from 140 to 160 °C for 15 min was attributed to the rapid decomposition of hemicellulose and lignin that resulted in a relatively increasing cellulose content with high thermal stability. The pre-exponential factor had a similar variation pattern with apparent activation energy, ranging from 24.56 to 36.86 min^{-1}.

Since the liquefaction condition of 180 °C/10 min provided the maximum liquefaction conversion yield with lowest content of liquefied residue and the minimum E_α, it was used as an optimal liquefaction condition to further investigate the pyrolysis properties of liquefied residues with conversion. It was worth mentioning that there was little or no correlation between $\ln(\beta/T_i^2)$ and $1/T_i$ when the pyrolysis conversion was less than 0.15 and greater than 0.55, in this study. The lack of correlation would introduce an erroneous interpretation of the phenomena. The linear regression lines are shown in Fig. 5, and the pyrolysis properties are presented in Table 4. The coefficients varied from 0.956 to 0.996, and the value of apparent activation energy was highly dependent upon conversion. The E_α gradually increased from 142.06 to 212.27 kJ mol^{-1} with the increase in conversion from 0.15 to 0.45, and then remarkably increased to 540.95 kJ mol^{-1} as the conversion reached to 0.55. It implied that the pyrolysis of liquefied residue was a complex process consisting of different degradation mechanism with pyrolysis conversion. The ln A_α increased with the increasing of conversion from 0.15 to 0.55, varying from 25.41 to 107.45 min^{-1}.

Table 4 E_α, ln A_α and coefficients (R^2) of liquefied residues from liquefaction condition of 180 °C/10 min obtained by the Kissinger method

α	Fitted equation	E_α/ kJ mol^{-1}	ln A_α/ min^{-1}	R^2
0.15	$y = 22.27 - 17087.40x$	142.06	25.41	0.9560
0.20	$y = 24.46 - 18293.92x$	152.10	27.36	0.9619
0.25	$y = 25.76 - 19174.69x$	159.42	28.71	0.9723
0.30	$y = 27.11 - 20073.86x$	166.89	30.11	0.9762
0.35	$y = 28.67 - 21092.99x$	175.37	31.72	0.9825
0.40	$y = 31.44 - 22796.72x$	189.53	34.56	0.9870
0.45	$y = 36.04 - 25585.56x$	212.72	39.28	0.9907
0.50	$y = 49.04 - 33229.73x$	276.27	52.54	0.9946
0.55	$y = 103.27 - 65064.76x$	540.95	107.45	0.9960

Conclusions

Thermogravimetric analysis of raw rape straw and liquefied residues indicated that the primary decomposition occurred in the temperature range of 280–390 °C. The hemicellulose decomposition peak was absent at the DTG curves of liquefied residues. The liquefied residue from 180 °C/15 min had the highest thermal stability under a high-temperature (>700 °C) condition among all liquefied residues. The maximum decomposition temperatures of liquefied residues shifted to higher temperature zones as the heating rate increased from 5 to 50 °C mol^{-1}. It suggested that the decomposition processes were delayed with the increasing heating rate. The rapid decomposition of hemicellulose and lignin during liquefaction contributed to the decrease in activation energy (E_α), whereas the recondensation reaction occurring at 180 °C/15 min remarkably increased the E_α. The lowest E_α was found in the liquefied residue from 180 °C/10 min. A noticeable increase in E_α was observed in the liquefied residue from the 180 °C/10 min condition with pyrolysis conversion, which suggested a complex decomposition process with the increasing of pyrolysis temperature.

Acknowledgements This work is funded by the USDA Forest Service 2015 Wood Innovations Funding Opportunity program, Agreement 15-DG-11083150-054. The authors also appreciate the financial support from the China Scholarship Council.

References

1. Xu JM, Xie XF, Wang JX, Jiang JC. Directional liquefaction coupling fractionation of lignocellulosic biomass for platform chemicals. Green Chem. 2016;18:3124–38.
2. Huang XY, Li F, Xie JL, De Hoop CF, Hse C-Y, Qi JQ, Xiao H. Microwave-assisted liquefaction of rape straw for the production of bio-oils. BioResources. 2017;12(1):1968–81.

3. Juhaida MF, Paridah MT, Hilmi MM, Sarani Z, Jalauddin H, Mohamad Zaki AR. Liquefaction of kenaf (*Hibiscus cannabinus* L.) core for wood laminating adhesive. Bioresour Technol. 2010;101(4):1355–60.
4. Xie JL, Qi JQ, Hse C-Y, Shupe TD. Effect of lignin derivatives in the bio-polyols from microwave liquefied bamboo on the properties of polyurethane foams. BioResources. 2014;9(1):578–88.
5. Feng JF, Jiang JC, Xu JM, Yang ZZ, Wang K, Guan Q, Chen SG. Preparation of methyl levulinate from fractionation of direct liquefied bamboo biomass. Appl Energy. 2015;154:520–7.
6. Doh GH, Lee SY, Kang IA, Kong YT. Thermal behavior of liquefied wood polymer composites (LWPC). Compos Struct. 2005;68:103–8.
7. Xie JL, Hse C-Y, Li CJ, Shupe TD, Hu TX, Qi JQ, De Hoop CF. Characterization of microwave liquefied bamboo residues and its potential use in the generation of nanofibrillated cellulosic fiber. ACS Sustain Chem Eng. 2016;4(6):3477–85.
8. Huang XY, De Hoop CF, Li F, Xie JL, Hse C-Y, Qi JQ, Jiang YZ, Chen YZ. Dilute alkali and hydrogen peroxide treatment of microwave liquefied rape straw residue for the extraction of cellulose nanocrystals. J Nanomater. 2017;. doi:10.1155/2017/4049061.
9. Damartzis T, Vamvuka D, Sfakiotakis S, Zabaniotou A. Thermal degradation studies and kinetic modeling of carbon (*Cynara cardunculus*) pyrolysis using thermogravimetric analysis (TGA). Bioresour Technol. 2011;102:6230–8.
10. Belotti G, Caprariis BD, Filippis PD, Scarsella M, Verdone N. Effect of *Chlorella vulgaris* growing conditions on bio-oil production via fast pyrolysis. Biomass Bioenergy. 2014;61:187–95.
11. Ceylan S, Topçu Y. Pyrolysis kinetics of hazelnut husk using thermogravimetric analysis. Bioresour Technol. 2014;156:182–8.
12. Niu M, Zhao GJ, Alma MH. Thermogravimetric studies on condensed wood residues in polyhydric alcohols liquefaction. BioResources. 2011;6(1):615–30.
13. Huang SW, Wu QL, Zhou DG, Huang RZ. Thermal decomposition properties of materials from different parts of corn stalk. BioResources. 2015;10(1):2020–31.
14. Slopiecka K, Bartocci P, Fantozzi F. Thermogravimetric analysis and kinetic study of poplar wood pyrolysis. Appl Energy. 2012;97:491–7.
15. Zhang ZP, He C, Sun TL, Zhang Z, Song KL, Wu QL, Zhang QG. Thermo-physical properties of pretreated agricultural residues for bio-hydrogen production using thermo-gravimetric analysis. Int J Hydrogen Energy. 2016;41(10):5234–42.
16. Zhao Y, Yan N, Feng MW. Thermal degradation characteristics of phenol-formaldehyde resins derived from beetle infested pine barks. Thermochim Acta. 2013;555:46–52.
17. Cai C, Zhang YH, Chen WT, Zhang P, Dong YP. Thermogravimetric and kinetic analysis of thermal decomposition characteristics of low-lipid microalgae. Bioresour Technol. 2013;150:139–48.
18. Borsoi C, Zimmernnam MVG, Zattera AJ, Santana RMC, Ferreira CA. Thermal degradation behavior of cellulose nanofibers and nanowhiskers. J Therm Anal Calorim. 2016;126(3):1867–78.
19. Song KL, Zhang H, Wu QL, Zhang Z, Zhou CJ, Zhang QG, Lei TZ. Structure and thermal properties of tar from gasification of agricultural crop residue. J Therm Anal Calorim. 2015;119:27–35.
20. Chen TJ, Li LY, Zhao RD, Wu JH. Pyrolysis kinetic analysis of three pseudocomponents of biomass-cellulose, hemicellulose and lignin. J Therm Anal Calorim. 2016;. doi:10.1007/s10973-016-6040-3.
21. Yang HP, Yan R, Chen HP, Lee DH, Zheng CG. Characteristics of hemicellulose, cellulose and lignin pyrolysis. Fuel. 2007;86:1781–8.
22. Zhang HR, Yang HJ, Guo HJ, Huang C, Xiong L, Chen XD. Kinetic study on the liquefaction of wood and its three cell wall component in polyhydric alcohols. Appl Energy. 2014;113:1596–600.
23. Kissinger HE. Reaction kinetics in differential thermal analysis. Anal Chem. 1957;29(11):1702–6.
24. Zhang HR, Pang H, Shi J, Fu TZ, Liao B. Investigation of liquefied wood residues based on cellulose, hemicellulose, and lignin. J Appl Polym Sci. 2012;123(2):850–6.
25. Brown ME, Dollimore D, Galwey AK. Reactions in the solid state. Amsterdam: Elsevier; 1980.
26. Tadini P, Grange N, Chetehouna K, Gascoin N, Senave S, Reynaud I. Thermal degradation analysis of innovative PEKK-based carbon composites for high-temperature aeronautical components. Aerosp Sci Technol. 2017;65:106–16.
27. Burnham AK. Computational aspects of kinetic analysis: Part D: the ICTAC kinetics project: multi-thermal-history model-fitting methods and their relation to isoconversional methods. Thermochim Acta. 2000;355:165–70.
28. Chetehouna K, Belayachi N, Rengel B, Hoxha D. Investigation on the thermal degradation and kinetic parameters of innovative insulation materials using TGA-MS. Appl Therm Eng. 2015;81:177–84.
29. Vyazovkin S, Burnham AK, Criado JM, Pérez-Maquedac LA, Popescud C, Sbirrazzuolie N. ICTAC kinetics committee recommendations for performing kinetic computation on thermal analysis data. Thermochim Acta. 2011;520(1–2):1–19.
30. Zhao H, Yan HX, Dong SS, Zhang Y, Sun BB, Zhang CW, Ai YX, Chen BQ, Liu Q, Sui TT, Qin S. Thermogravimetry study of the pyrolytic characteristics and kinetics of macro-algae *Macrocystis pyrifera* residue. J Therm Anal Calorim. 2013;111:1685–90.
31. Chirayil CJ, Joy J, Mathew L, Mozetic M, Koetz J, Thomas S. Isolation and characterization of cellulose nanofibrils from *Helicteres isora* plant. Ind Crops Prod. 2014;59:27–34.
32. Liang YG, Cheng BJ, Si YB, Cao DJ, Jiang HY, Han GM, Liu XH. Thermal decomposition kinetics and characteristics of *Spartina alterniflora* via thermogravimetric analysis. Renew Energy. 2014;68:111–7.
33. Girisuta B, Janssen LPBM, Heeres HJ. Kinetic study on the acid-catalyzed hydrolysis of cellulose of levulinic acid. Ind Eng Chem Res. 2007;46:1696–708.
34. Gai C, Dong YP, Zhang TH. The kinetic analysis of the pyrolysis of agricultural residue under non-isothermal conditions. Bioresour Technol. 2013;127:298–305.